Contrails MS 36

Patrick Minnis

Submitted to
Encyclopedia of Atmospheric Sciences, 2nd Edition

Contact: Dr. Patrick Minnis, Science Division, MS 420, NASA Langley Research Center, Hampton, Virginia 23681 USA, email: Patrick.Minnis-1@nasa.gov

Synopsis: Contrails are anthropogenically induced clouds that have the potential to impact climate and reveal aircraft positions. Contrail formation is governed by temperature and humidity fields and is generally limited to temperatures below –40°C. Contrail growth and transformation into cirrus clouds is more complex and must be understood to fully account for contrail effects on climate. Contrail microphysical and optical properties as well as coverage, location, and illumination conditions are also critical for determining contrail radiative forcing, a climate change metric. In situ measurements, satellite remote sensing, cloud process models, and climate models are used to study contrails and their potential impacts on global climate.

1. 0 Introduction

One of the most visible anthropogenic effects on the atmosphere is the condensation trail, or contrail. These aircraft-induced clouds have become a common sight since the 1960's because of increasing jet traffic, but were observed as early as 1919. Contrails were frequently seen and filmed during World War II during bombing raids or dogfights. They were briefly studied in Germany during the war but drew little scientific interest again until the early 1950's when the use of jet aircraft by military and commercial aviation accelerated. Interest waned with only sporadic studies until the 1990's when aircraft exhaust and contrails became the foci of numerous research efforts. Concerns over their impact on climate and aircraft visibility have been the primary motivation for the recently intensified research into contrails. Climate researchers are interested in knowing whether they cause warming or cooling of the atmosphere, while military mission planners would prefer that contrails do not reveal the positions or paths of their aircraft. Understanding contrail effects requires knowledge of their physical and optical characteristics and how, when, and where they form.

2.0 Contrail formation

Contrails are generally composed of ice crystals with trace amounts of exhaust products such as soot and sulfates. The contrail ice crystals form because the relative humidity with respect to liquid water U_w temporarily reaches the saturation point in the plume mixture of ambient air and hot exhaust gases. Tiny droplets develop on background aerosols or on aerosols formed by exhaust compounds. Because the ambient temperatures required for contrails are

generally colder than –40°C, the small water droplets instantly freeze and grow via vapor-to-ice deposition as long as the relative humidity with respect to ice U_i remains above 100%. They dissipate via sublimation if U_i is below the saturation point or by precipitation into unsaturated layers below the flight level.

2.1 Aerodynamic contrails

Another type of contrail that forms at higher temperatures is the aerodynamic contrail that forms behind the tips or the leading edges of aircraft wings. These are commonly seen emanating from subsonic aircraft in humid atmospheres, usually at low levels. In these cases, the ambient air is compressed at the wing tip and then expands quickly during adiabatic expansion within the low-pressure area above the wing tip. The expansion temporarily cools the air sufficiently so that it falls below the dewpoint resulting in condensation. Aerodynamic contrails are most commonly seen at low altitudes where they form short-lived liquid water contrails. Sometimes, at temperatures slightly greater than -40°C, they can form ice crystal trails that will persist if the air is supersaturated with respect to ice. Modeling studies indicate that they are likely to be important in tropical latitudes where cruising altitudes more often at temperatures slightly greater than -40°C. Because ice contrails generated from aircraft exhaust are the more common variety, aerodynamic contrails are not considered any further here.

2.2 Exhaust contrails

The basic concepts for determining the conditions for contrail formation were independently developed by E. Schmidt in Germany during 1941 and H. Appleman in the USA during 1954. The lines in **Fig. 1** schematically illustrate the ice contrail formation process for several scenarios with the ambient temperatures T_a and water vapor partial pressures e_a indicated by the points at the lower end of each line. Each line extends to the temperature T_e

and water vapor partial pressure e_e of the exhaust exiting the engine. As the exhaust gases mix with the ambient air, the mean temperature and moisture properties of the mixture follow these

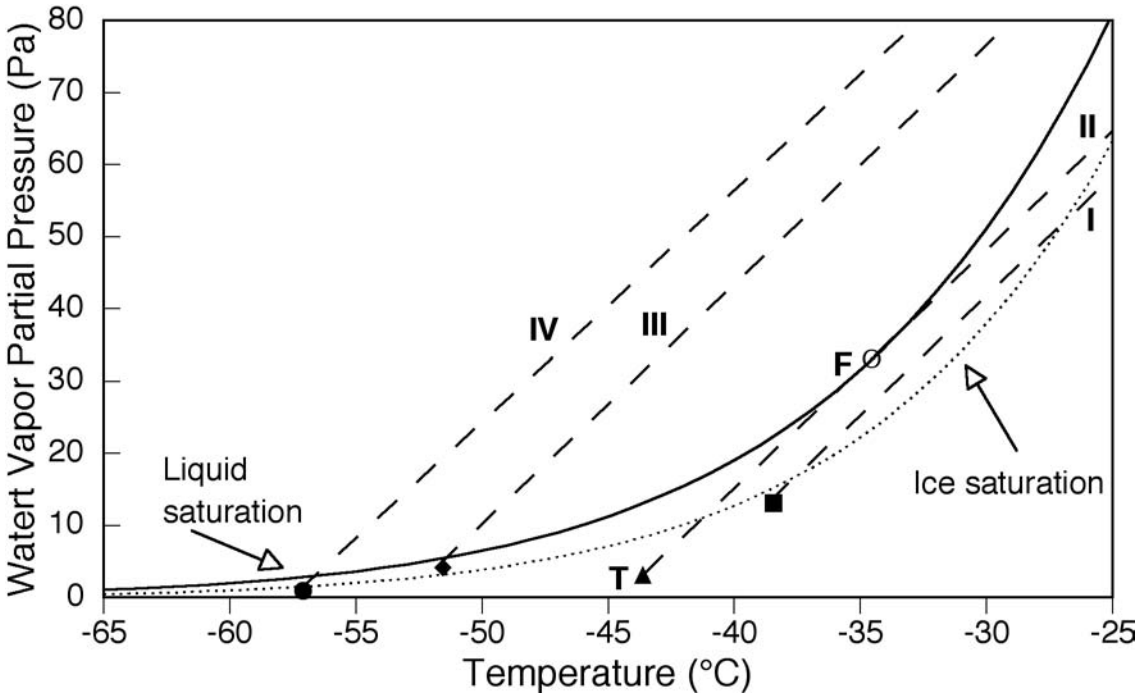

Figure 1 Phase diagram with mixing lines for aircraft exhaust in different ambient conditions.

mixing lines until they approach the ambient conditions. In cases defined by the lines I, II, and IV, the ambient water vapor pressure is less than the ice saturation partial pressure e_I, while in case III, $e_a > e_I$. In case I, the partial pressure exceeds e_I during the mixing but never reaches water saturation and a contrail does not develop. A short-lived contrail would develop in case II because at point F, the mixture temperature T_F coincides with the liquid water saturation partial pressure e_w. The contrail would form when the plume temperature reached T_F and persist until the plume partial pressure decreased to a value below e_I at approximately –42°C. A long-lived, persistent contrail would form in Case III because the ambient air is supersaturated with respect to ice. Because saturation conditions cover a greater range of temperatures after initial formation, the contrail formed in Case IV would probably last longer than that in Case II.

Although contrail formation has been observed at temperatures as great as –36°C, it is clear from **Fig. 1** that contrails form much easier at lower temperatures. The threshold temperature T_T for contrail formation is defined as the warmest ambient temperature that will support contrail formation for a given value of e_a and the exhaust parameters T_e and e_e. The latter quantities determine the mixing line slope G and are a function of engine type, operating conditions, and fuel, while the value of e_a can be determined from vertical profiles of atmospheric and dew point temperatures. In case II, the ambient temperature at point T is the contrail formation threshold temperature for the given values of e_a and the mixing line slope G. That is, the ambient temperature enabling contrail formation temperature would have to change if either e_a or G varied and, therefore, T_T is unique for each pair of e_a and G. The threshold temperatures are greater than T_a for cases IV and III, and less than T_a for case I. To find T_T for a particular slope and e_a, it necessary to determine the tangent point T_F for a line having slope G with the curve describing the variation of e_w with T. Given a value of G, the threshold temperature can be computed for T_F between -10°C and -60°C using

$$T_F = -46.46 + 9.43 \ln(G - 0.053) + 0.720[\ln(G - 0.053)]^2, \qquad [1]$$

where G is given in Pa K^{-1}. The threshold temperature for any value of U_w or e_a can be determined iteratively with

$$T_T = T_F - [e_w(T_F) - U_w e_w(T_T)] / G. \qquad [2]$$

The mixing line slope depends on the specific plume enthalpy h_p and the water vapor mixing ratio q, which, in turn, are related to the emission index EI_w, mass specific combustion heat Q, and the overall engine efficiency η. Specifically,

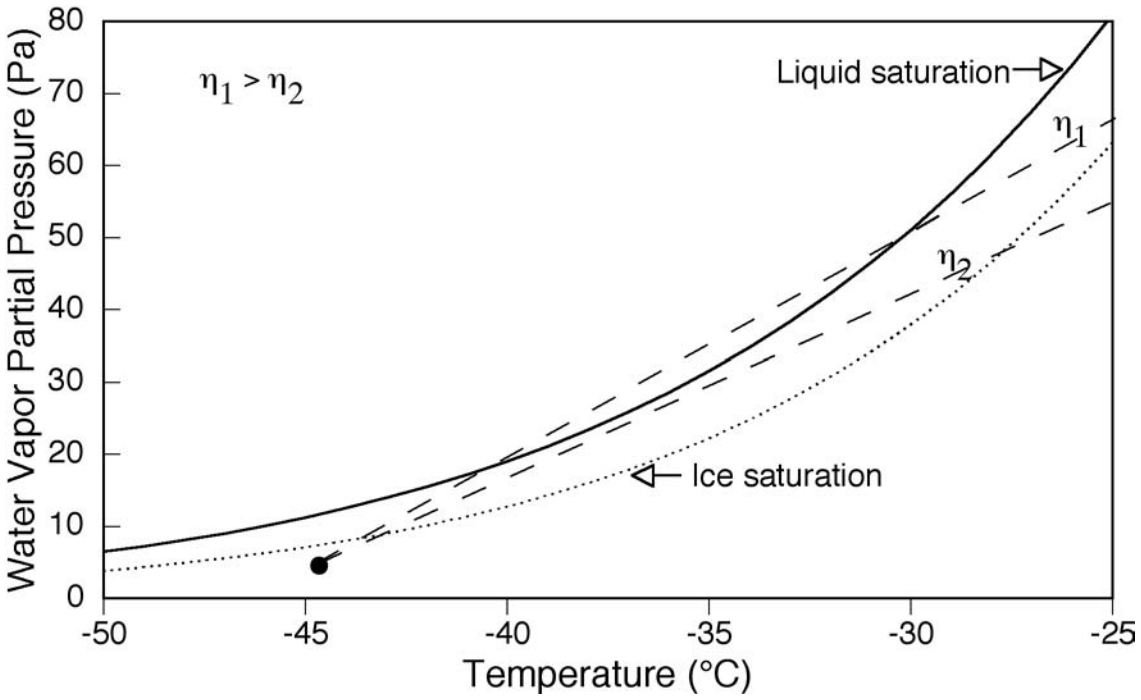

Figure 2 Hypothetical mixing lines for different propulsion efficiencies.

$$G = \Delta e/\Delta T = [\Delta q/\Delta h_p]pc_p/\varepsilon = EI_w pc_p/[\varepsilon Q(1-\eta)], \qquad [3]$$

where c_p is the specific heat capacity, p is the pressure, and $\varepsilon = 0.622$. The emission index, the mass of water produced per mass of combusted fuel, accounts for Δq since $e_e >> e_a$. The enthalpy differential is also determined almost entirely by Q and η because the ambient heat is negligible compared to that produced by the engine. Since Q and EI_w can be determined for a given fuel, then the overall efficiency, the ratio of propulsion energy to total combustion energy, is the primary variable affecting the mixing line slope. The slope of the line increases with

increasing efficiency. Each type of engine has a nominal efficiency that is based on stationary operating conditions. The overall efficiency, however, may vary for a given engine because of different airframes, maintenance, and operating conditions. **Figure 2** illustrates the impact of efficiency for a given set of ambient conditions. In this instance η_2 is slightly less than η_1 resulting in a contrail from the plane with η_1 and no contrail from the one with η_2. Thus, two planes flying in the same environment can produce two different results. Similarly, a plane might produce a contrail when it is cruising but not when it is ascending, depending on the effect of acceleration on the efficiency.

Contrails typically form at a distance of about 30 m or less behind the aircraft engines where the turbulent mixing has sufficiently reduced the temperature. The latest research results indicate that the initial condensation of the supercooled droplets takes place on a wide variety of particles including exhaust products. e.g., sulfate aerosols, soot, and metallic particles as well as ambient mineral aerosols. When the contrails are about 1 minute old, the mean particle radius is around 2 μm and increases up to 4-5 μm after 3 minutes. A wide variety of particle shapes have been observed in young contrails including hexagonal columns and plates, triangles, irregular forms, and spheroids. Young contrails often appear saw-toothed or appear to have a cellular structure that results from the wake vortices formed by the aircraft. The wake vortex pairs act to extend the contrail vertically with irregularities that can lead to formation of local convective cells or radiative cooling gradients that aid mixing of the contrail with the ambient air.

3.0 Contrail Growth and Structure

Once formed, a contrail develops or dissipates in the same manner as a naturally generated cirrus cloud. Contrail growth and spreading depend on the thickness of the

supersaturated layer, the degree of ice supersaturation, the nature of the wake vortex, and the wind velocity and shear. When contrails persist, the particles typically grow to lengths from 30 - 1000 μm, sizes usually associated with natural cirrus clouds. Ice particle growth is rapid in

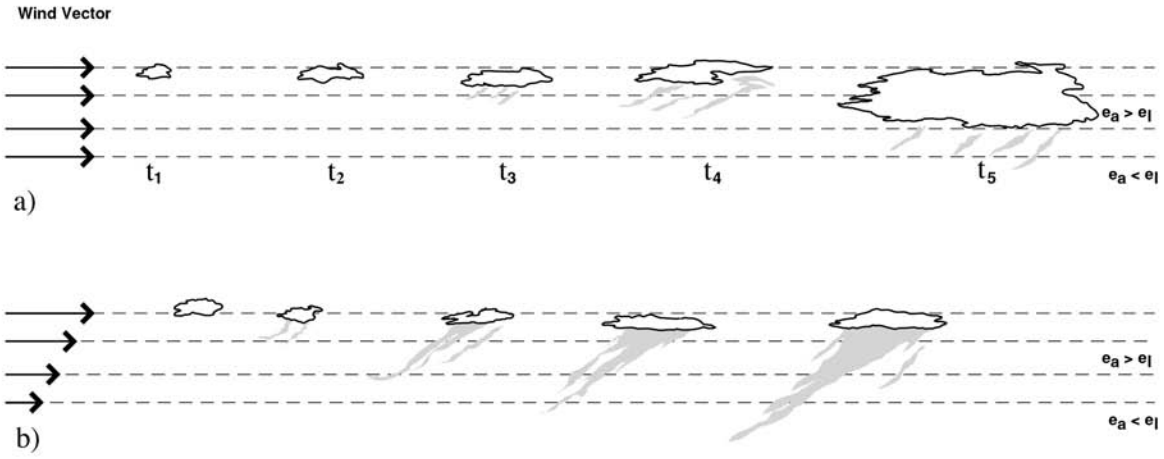

Figure 3 Schematic depiction of contrail spreading in conditions with and without wind shear.

highly supersaturated layers and results in fall streaks that spread horizontally in lower layers according to the wind shear. **Figure 3a** shows a cross-section view of a hypothetical persistent contrail growing and spreading in the absence of vertical wind shear. When wind shear is present (**Fig. 3b**), the contrail may spread mostly by turbulent mixing induced by the aircraft vortex or by radiative processes. It may also thicken by turbulence or through precipitation. If the crystals fall into supersaturated air below, they will continue to grow or, possibly, split into additional crystals. The linear shape of the contrail will be distorted and the contrail will soon look like a natural cirrus cloud to the observer.

An example of this shear effect is seen in **Fig. 4**, which shows the cross-sectional growth of a contrail observed with a surface-based scanning lidar. After 1.1 min (**Fig. 4a**), when the vortex effect is dissipating, the overall width of contrail is only ~160 m compared to its vertical

depth of roughly 260 m. It grows progressively wider during the following 14 min reaching a horizontal extent of 1 km (**Fig. 4d**). As it widens, the lower part of the contrail starts evaporating (**Fig. 4b**) in the dry layer below the 10.35-km level, while the upper portion slowly rises due to

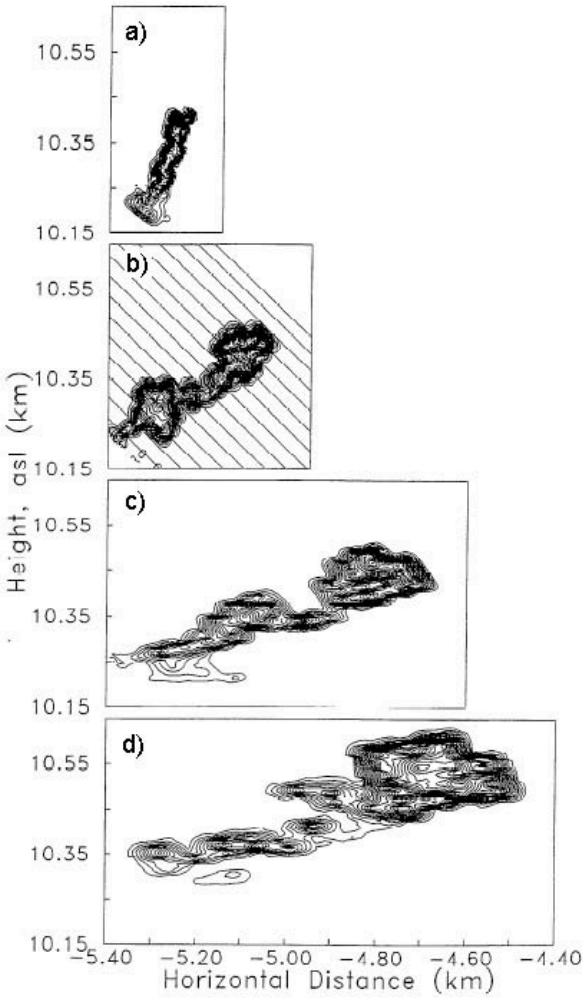

Figure 4. Contour plots of the lidar backscatter signal of cross-sections of a contrail. Age of contrail: (a) 1.1. min, (b) 6.2 min, (c) 10.9 min, and (d) 15.5 min. (Adapted from Fig. 2 of Freudenthaler et al. (1995).

the buoyancy resulting from the release of latent heat into the air from the condensation-freezing process producing the ice particles. The wind mean vertical wind shear for this case was ~4 m s^{-1} km^{-1}.

Contrails that are older than several hours are often indistinguishable from natural cirrus clouds regardless of shear conditions. Most studies indicate that the number of crystals in a contrail remains essentially constant after formation in supersaturated conditions. Thus, if the contrail precipitates, the contrail cloud at flight level might gradually fade as its particles are depleted. If e_a is just above ice supersaturation, then the crystal growth will be limited and little precipitation occurs. In this case, the contrail may spread slowly by diffusion, maintaining its linear shape for a relatively long time. Because the crystals grow by deposition, the amount of ice water in the contrail increases until the particles fall out or equilibrium is reached between the ice water content and e_I. Such equilibrium conditions generally do not last very long and the contrail eventually dissipates. Although most persistent contrails observed from satellites have visible optical depths between 0.10 and 0.4, the values are highly variable ranging between 0.01 and 2. Optically thin contrails may occur frequently but most cannot be detected in satellite imagery. The lifetimes of contrails are also extremely variable. Short-lived contrails may only last a few seconds while some contrail-generated cirrus clouds have been tracked for more than 17 hours. The shape, size, optical properties, and life cycle of contrails are highly dependent on their environment, so that a multitude of contrail morphologies can occur. Contrail-cirrus clouds are generally similar to natural cirrus clouds within a few hours after their formation.

Because water vapor and temperature are not homogeneously distributed, even at relatively small scales (~100 m), contrails may form or persist in an apparently erratic fashion as shown in **Fig. 5**. For example, an on-off pattern can occur as an aircraft flies through a moist layer disturbed by a vertical wave or even weak convective plumes. The contrails in **Fig. 5a** form in the ascending parts of the wave or plume where the temperature of the rising air drops below the threshold temperature, while in the descending portions the air warms and dries

resulting in no contrail formation. Similar patterns can result from a plane ascending or descending plane through several thin layers that are near saturation but separated by dry layers as in **Fig. 5b**. The persistence of a contrail or parts of it depends on the value of e_a relative to e_i along the contrail line. Thus, parts of a contrail may rapidly dissipate while other portions may

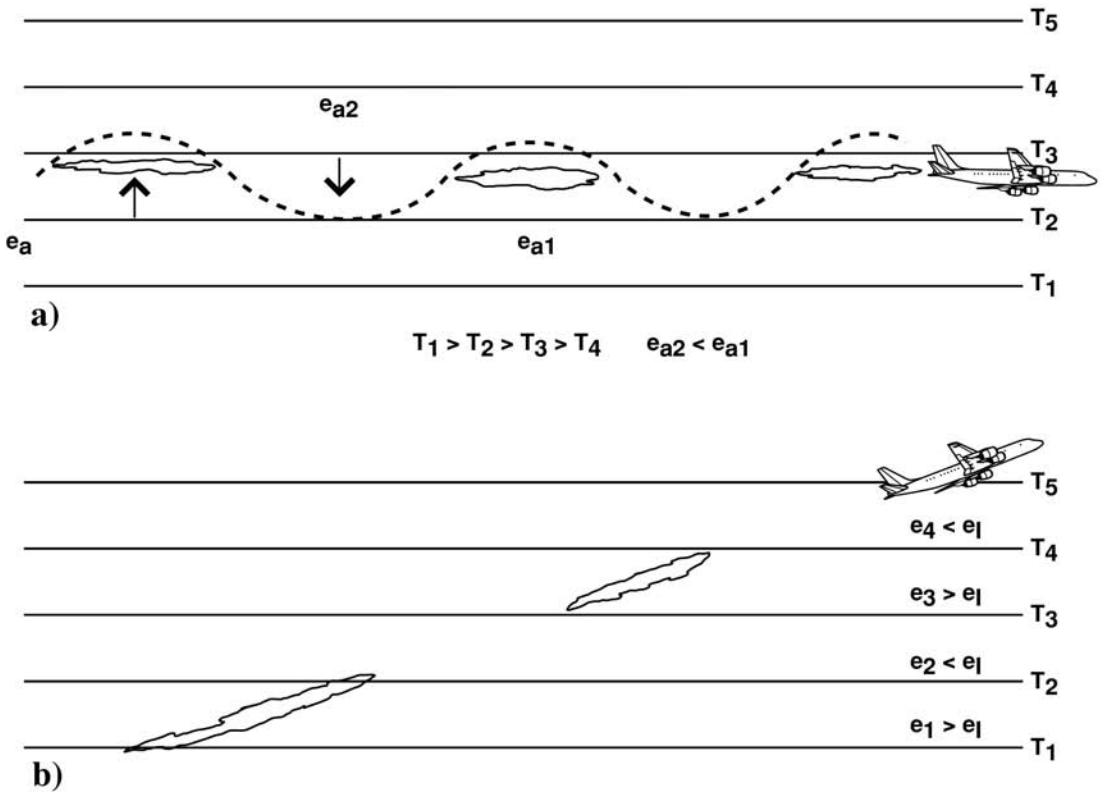

Figure 5 Schematic depiction of contrails forming in an on-off pattern.

linger and even grow. The local turbulence induced by the airframe, the atmospheric stability, and the wind vector also affects the morphology of the contrail.

Photographs of the most familiar type, short-lived contrails, are shown in **Fig. 6**. In both cases, the trails gradually fade without much spreading. In those situations, e_a is only slightly less than e_I. When e_a exceeds e_I, less familiar shapes can occur. In the top panel of **Fig. 6**, the contrail dissipates several kilometers behind the aircraft. The lower panel shows several intermittent

contrails (e.g., **Fig. 5**) that persisted for less than an hour with little spreading. **Figure 7** shows examples of contrails at different stages of growth or persistence at the same time in different parts of the sky. East of the observer (**Fig. 7a**), the contrails appear to maintain their linearity in the foreground except for the curved contrail crossing many of the other contrails. Toward the

Figure 6 Short-lived contrails.

horizon, it appears that the contrails have spread out and lose some of their linearity, looking more like natural cirrus. One contrail appears to be segmenting. To the south (**Fig. 7b**), a succession of slowly spreading contrails extends off to the hazy horizon. Different parts of these contrails spread differently with the sections near the center of the photograph shifted and twisted slightly compared to the rest of the contrail segments. Many of these contrails persisted for at least several hours before advecting southeastward out of view.

Condensation trails often form ahead of advancing fronts in the poleward flow of an upper level trough where conditions are not quite saturated enough for natural cirrus development. In these instances they can occur at multiple levels in the atmosphere because the formation conditions often cover a large depth of the atmosphere and air traffic uses a wide range

of altitudes. But they also form in a variety of other conditions. In **Fig. 7**, the contrails formed from moisture advecting westward from the high altitude outflow of an occluding low pressure system approximately 1400 km west of the observer. The atmosphere was saturated with respect to ice at temperatures below -40°C in many layers between 9.9 km (32.7 kft) and 13.1 km (43.2

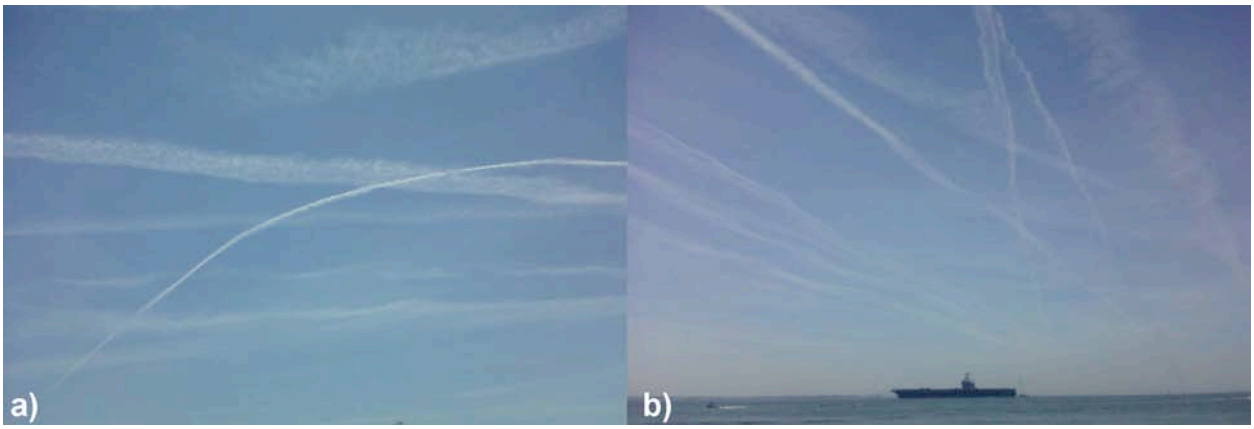

Figure 7 Persistent contrails in various stages of growth and decay as seen (left) east and (right) south of Ft. Monroe, VA at 1625 UTC, 21 May 2010.

kft). Thus, the formation of crossing contrails, which only occur because planes fly at different flight levels depending on flight path direction, is likely for this case because of the depth of the saturated layers.

The contrails seen in **Fig. 7** are part of a larger area of contrails that is evident in infrared images (**Fig. 8a**) from the MODerate-resolution Imaging Spectroradiometer (MODIS) on the Terra satellite. These images were taken around the same time as the photograph in **Fig. 7**. Subsequent imagery shows that these contrails dissipated downstream to the east while additional contrails formed within or beneath the advancing thin cirrus clouds.

Contrails can form within cirrus clouds where they are manifest by reduced particle sizes or local thickening of the cloud. Aircraft exhaust can also affect supercooled liquid water clouds that have temperatures below the threshold value. When a plane flies through this type of cloud, the dynamic pressure changes due to flow over the wing edges or behind propeller tips causes

cooling sufficient to freeze the surrounding cloud droplets. The thermodynamic equilibrium shifts from a vapor-to-liquid to vapor-to-ice process causing a rapid depletion of the available water vapor onto the frozen droplets. Newly formed ice crystals quickly grow large enough to fall out of the cloud resulting in a streak below the cloud and a gap within in the cloud.

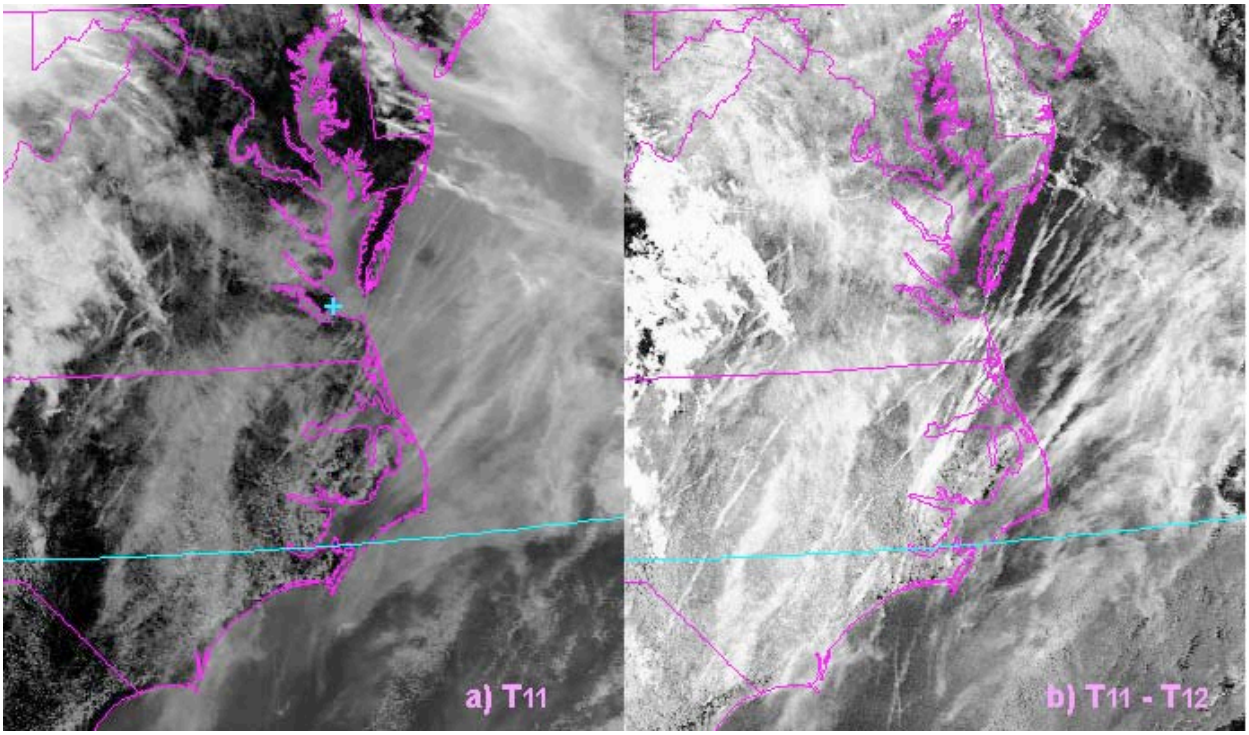

Figure 8 Infrared temperature and temperature difference images of contrails over Maryland, Virginia, and North Carolina, USA from the Terra 1-km resolution MODIS at 1615 UTC, 21 May 2010. Cross indicates position of observer in **Fig. 7**.

This gap, called a distrail, hole punch cloud, or canal cloud, is linear when the plane flies for an extended distance within the cloud or oval shaped when the aircraft is briefly inside the cloud as it ascends or descends. Depending on the conditions, especially the original cloud thickness, a distrail will either persist or be filled in with a new water droplet cloud. In very moist conditions, significant snowfall can occur along the path of the aircraft. Distrails are most frequently observed in altostratus or altocumulus clouds.

4.0 Contrail Remote Sensing

Although contrails are most often identified by their linear shapes both from ground observations (**Fig. 7**) and satellite imagery (**Fig. 8**), these man-made clouds can take on other geometric shapes according to the particular flight patterns and winds. For instance, spiral shapes result from a plane in a circular holding pattern within an advecting supersaturated layer, while a figure eight can form in a similar layer if the plane flies a linear holding pattern. The linear structure is most common and forms the basis for automated identification of contrails. Because detection of contrails is important for various scientific applications, methods have been developed for differentiating contrails from other linear clouds in satellite imagery, the only plausible data source for studying the spatial and temporal distribution of contrails and their physical characteristics. Automated techniques for contrail detection typically create an image of a parameter most likely to be associated with a contrail, then apply a variety of image processing methods to find linear structures within that image.

Such methods, which are still being researched, usually take advantage of the relatively distinct infrared optical properties of younger contrails to compute a parameter that is likely to yield a distinctive contrail signal for image processing. Because of their relatively small size (mean effective radii between 5 and 25 μm), the ice crystals in contrails have single-scattering albedos that increase more with decreasing wavelength λ in the thermal infrared region (3.5 - 15 μm) than the single-scattering albedos of larger particles typically found in most cirrus clouds (effective radii greater than 15 μm). Thus, contrails usually transmit more radiation at shorter infrared wavelengths than a cirrus cloud of equivalent optical depth, resulting a signal that often reveals a contrail.

To better understand this effect, consider that the satellite measures a spectral radiance L_λ that is recorded as a brightness temperature T_λ, which is proportional to λ through the Planck function. For a cloud or contrail the observed radiance can be modeled simply as

$$L_\lambda = \varepsilon_\lambda L_c + (1-\varepsilon_\lambda) L_b, \qquad [4]$$

where L_c is the radiance emitted at the cloud temperature T_c, L_b is the upwelling radiance at the cloud base with an equivalent brightness temperature T_b, and ε_λ is the cloud emissivity. In general, $L_b > L_c$, so that an increase in cloud transmissivity, $(1-\varepsilon_\lambda)$, results in more transmission of L_b and a larger value of L_λ. Thus, T_λ will be greater at shorter wavelengths than at longer ones as long as the cloud is optically thin (ε less than 0.9 or so). This effect can be seen in **Fig. 8**, which shows the 11-μm temperature (T_{11}) image and an image of brightness temperature difference ($T_{11} - T_{12}$) between the 11- and 12-μm channels of the Terra MODIS. Some of the contrails are readily apparent in the 11-μm image (**Fig. 8a**) but are obscured by other cirrus clouds. The temperature difference image in **Fig. 8b** reveals many contrails that were not evident in the standard infrared image and highlights others more clearly. Even the curved contrail in Fig. 7a can be seen crossing over some of the parallel contrails east of the observer's location in **Fig. 8b**. Because the actual temperature difference contrast depends on the effective particle sizes and optical depths of the surrounding clouds, and those quantities are naturally variable, the contrails are not always detected. Furthermore, other features like cirrus streaks, coastlines, or cloud edges, may produce similar signals.

When T_b is not very different from T_c, such techniques do not reveal the contrails very readily because the signal is so small. Therefore, contrails imbedded in relatively thick cirrus

clouds cannot be seen in most temperature difference imagery. However, during the daytime, contrails can often be detected using temperature differences between a channel near 11 μm and one in the shortwave-infrared wavelength range (3.5 - 4.5 μm). At those wavelengths, the satellite imagers measure an emission component and a solar-reflected component. The smaller contrail ice crystals reflect more sunlight than the surrounding cirrus crystals resulting in a relatively large brightness temperature. **Figure 9** shows MODIS imagery for the same case as in **Fig. 8**, except that it is shifted westward covering parts of Ohio, Pennsylvania, Virginia, and West Virginia. The 11-μm image in **Fig. 9a** shows little sign of contrails, particularly in the thick cirrus over Ohio, Pennsylvania, and West Virginia, while the $T_{11} - T_{12}$ image (**Fig. 9b**) reveals a few contrails over those same areas. The 11 and 3.7-μm temperature difference ($T_{3.7} - T_{11}$) image (**Fig. 9c**), however, reveals a large number of linear contrails around the common borders of those states. These contrails are absent or faint in **Fig. 9b**. Conversely, where thick cirrus is absent (e.g., south central Virginia), the contrails are more prominent in **Fig. 9b** than in **Fig. 9c**. Thus, the two images tend to complement each other with respect to contrail detection. Further enhancement of the photograph would likely reveal more contrails in the temperature difference images. Again, the ability to detect contrails in a thick cirrus cloud depends on many factors including the contrail age and its relative depth in the cloud as well as the particle sizes in the cirrus cloud, and the viewing and illumination conditions. To date, the $T_{3.7} - T_{11}$ information has not been employed to monitor contrails for climate purposes since it is applicable only during the daytime, and contrails imbedded in thick cirrus clouds will likely have minimal radiative impact.

Contrails can also be detected in high-resolution visible and near-infrared imagery in certain conditions. For example, when not imbedded in cirrus or over lower clouds, a young

contrail is often reflective enough to be seen as a bright line in a 1-km visible channel image. Sometimes, the contrail will cast a shadow on lower clouds and can be detected from its shadow. Near-infrared channels on or near water vapor absorption lines, like that near 1.38 μm, often do

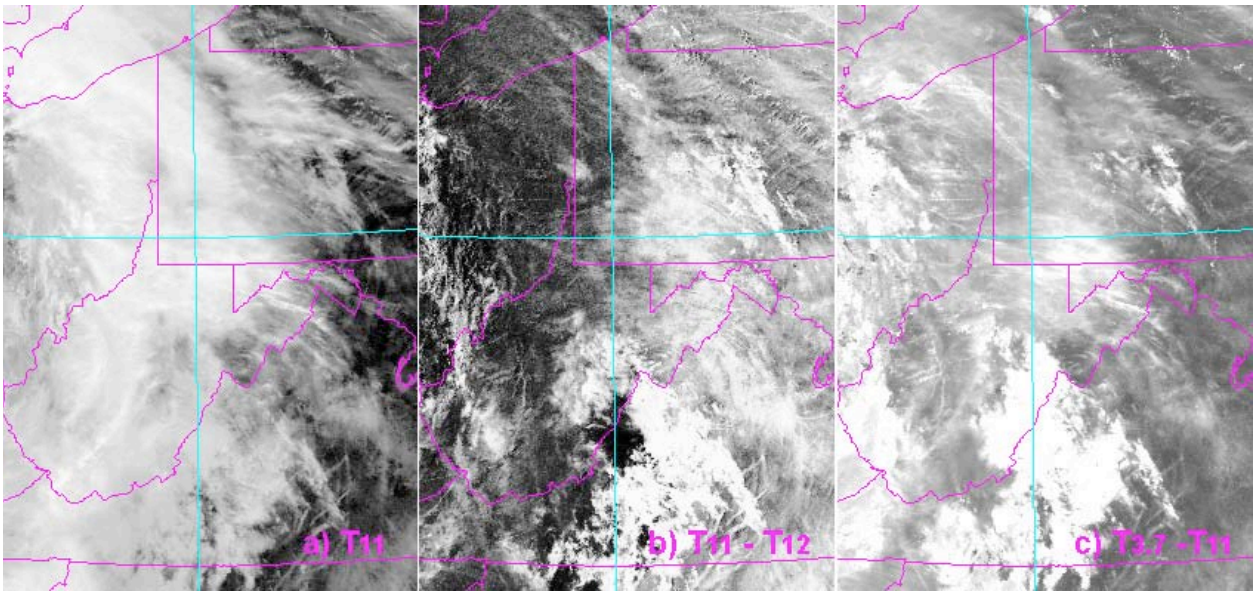

Figure 9 Contrails imbedded in thick cirrus over Ohio, Pennsylvania, Virginia, and West Virginia from the Terra 1-km resolution MODIS at 1615 UTC, 21 May 2010.

not receive any significant reflectance from lower clouds so that even very thin high clouds, such as contrails, can be detected.

Figure 10 shows an example of a contrail outbreak over Florida at 1600 UTC, 23 March 2011 as seen in Terra MODerate-resolution Imaging Spectroradiometer (MODIS). Very faint contrails can be seen west of the peninsula in the true color image (**Fig. 10a**) with little indication of contrails near the Georgia-Florida border. The 1.38-μm reflectance image (**Fig. 10b**) reveals a mass of crossing contrails along the border and fine detail of the contrails and contrail-cirrus over the whole area. The spread of the contrails and cirrus clouds is greater in **Fig. 10b** than in the true color image (Fig. 10b) or the $T_{11} - T_{12}$ image (**Fig. 10c**). When there are no underlying clouds, the 1.38-μm channel can reveal contrails with very small optical depths, which modeling studies suggest are quite common but are not seen in infrared imagery. Although potentially

promising for more accurate monitoring of contrails, the 1.38 μm and other near-infrared channels are only applicable during the daytime and are strongly affected by underlying clouds. Thus, thermal infrared channels are mainly used for monitoring contrails.

Contrail properties such as temperature, height, optical depth, and effective particle size can be determined with the same methods used to remotely sense cloud properties from satellite imager data. Such techniques typically require multispectral imagers that can be used to simultaneously solve for ε, T_c, and the particle size. When an insufficient multispectral radiance set is available, one or more of the parameters must be assumed to obtain a solution for the other parameters. These methods generally provide results consistent with in situ measurements. Satellite analyses have found mean optical depths that average approximately 0.11 over Europe and 0.25 for the USA. Modeling studies show similar discrepancies between contrails over the USA and Europe, but some have also indicated that the satellite retrievals miss large numbers of contrails having optical depths smaller than 0.05. The average temperature of contrails detected from satellite data over the midlatitudes is -54°C, which corresponds to an average pressure of about 200 hPa.

5. 0 Contrail-Cirrus

An increase in cirrus cloudiness because of contrail formation has been hypothesized since the beginning of the commercial jet age. The possibility for enhanced cirrus coverage resides in the frequency and extent of areas that are ice supersaturated. In situ measurements and numerical model analyses have shown that e_a exceeds e_i 10 - 20% of the time in air at flight altitudes (8 - 12 km). Thus, the potential exists for substantial increases in cirrus coverage over

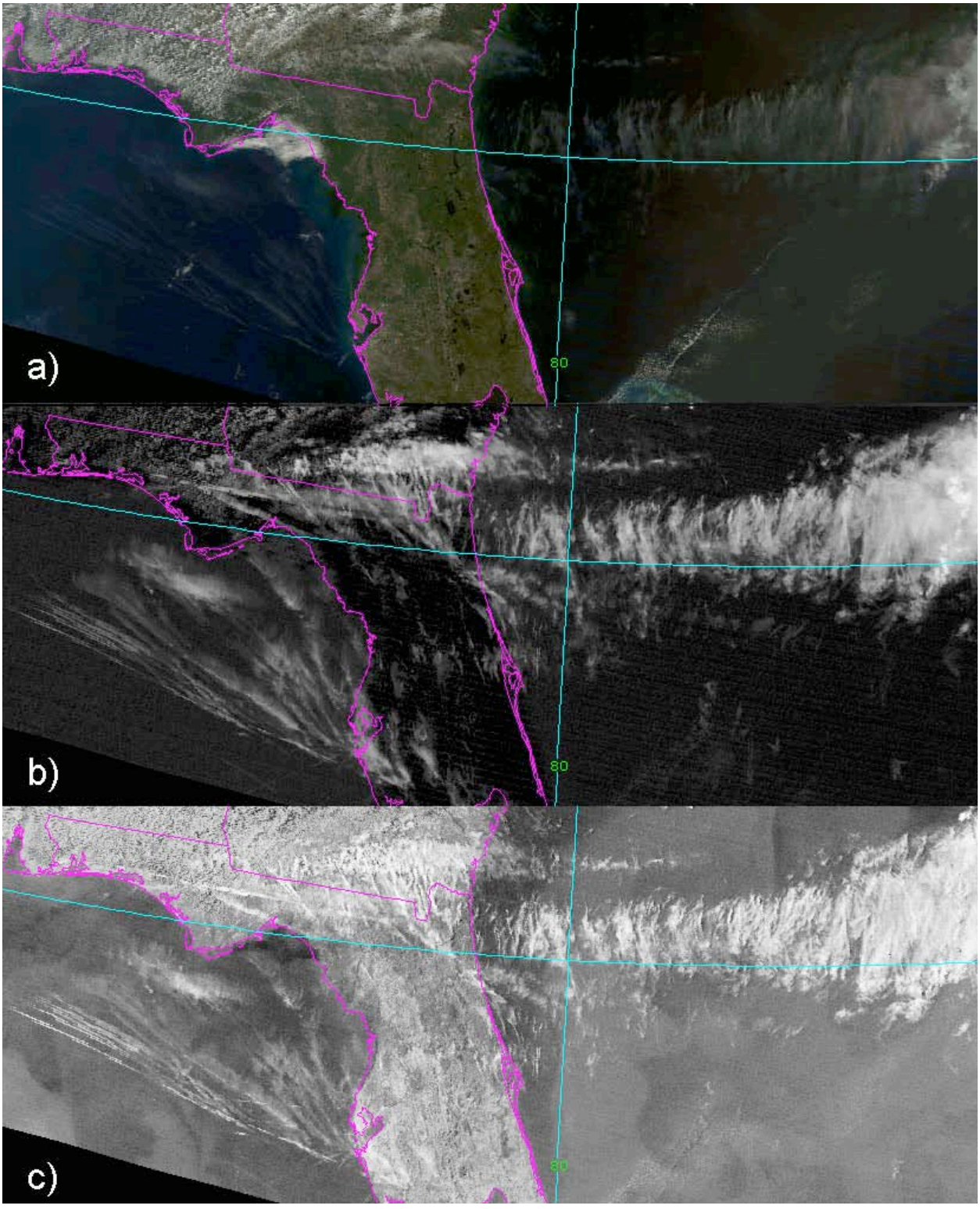

Figure 10 Terra MODIS 1-km imagery taken 1600 UTC, 23 March 2011. (a) true color, (b) 1.38-μm reflectance, and (c) T11 – T12.

areas crossed by air traffic. Because the stratosphere is generally very dry, aircraft flying above the tropopause generates few contrails, especially persistent ones.

The conditions necessary for supporting contrail formation at flight altitudes change with the seasons. Over midlatitude areas, contrail conditions are favorable most often during winter and early spring when the troposphere is coldest. During summer, the temperatures at flight levels are often too high to enable contrail initiation. Over areas poleward of about 50° latitude, the tropopause is often below flight level during winter, so that a significant number of planes fly in the stratosphere resulting in contrail suppression. Conditions are more favorable for contrails during the summer and autumn in the subarctic regions. In the tropics, the altitude for contrails is generally above 11 km year round, so the potential for contrail formation is reduced for many commercial planes. However, persistent contrails are likely to occur more frequently in the tropics than at other latitudes at altitudes above 11 km because of more abundant water vapor.

Surface observations over the USA during the 1990's indicate that persistent contrails occur, on average, approximately 9% of the time, but the frequency varies from less than 5% in low traffic areas to 25% in the main air corridors. Approximately 80% of these persistent contrails are either imbedded in, extending from, or near natural cirrus clouds. Contrail coverage has been derived from satellite imagery only for those contrails that are linear and large enough to detect in 1-km infrared data. Satellite-based estimates of daily mean contrail amounts over central and western Europe, the North Atlantic, the conterminous USA, Japan, and Thailand are approximately 0.5, 1.0, 0.5, 0.3, and 0.1%, respectively, and, for the early 1990's, roughly 0.1% globally. Similar as well as much smaller or larger values have been derived from theoretical calculations using realistic air traffic patterns, numerical analyses of meteorological fields, and

specified engine efficiencies. However, uncertainties in detecting contrails unambiguously with automated satellite image analysis techniques are still quite large,

Automated detection and assessment of contrail coverage has been confined to contrails that are identifiable by their linear structure and small particle sizes. Because these identifying features are often lost as the contrails spread, the linear contrail coverage estimates represent the minimum amount of the sky that is covered by contrails. The $T_{11} - T_{12}$ images (**Fig. 11)** from the Advanced Very-High Resolution Radiometer (AVHRR) on the NOAA-16 and NOAA-19 satellites illustrate the difficulty of distinguishing contrails from cirrus clouds. The large area of cirrus clouds seen east of north Florida in **Fig. 10b** began as hundreds of linear contrails north of the Florida peninsula at least 3 hours earlier (**Fig. 11a**). Those west of Florida were already quite wide at 1256 UTC and extended as far west as Louisiana. The latter group dissipated by 1735 UTC (not shown), while the former mass of contrails persisted as a collection of nearly contiguous cirrus clouds over the Atlantic with a few scattered linear features (**Fig. 11b**). Without following the linear contrails seen in **Fig. 11a**, it would be impossible to differentiate the contrail cirrus over the Atlantic in **Figs. 10b** and **11b** as separate from naturally forming cirrus clouds.

Geostationary satellite data can be used to track some contrails as they grow and change in shape and composition. Examination of the geostationary data (not shown) taken during 23 March 2011 revealed that the large contrail mass over the Atlantic actually started forming as early as 1145 UTC over north Georgia and South Carolina and did not completely dissipate until 2345 UTC. The long contrails west of Florida started forming over Louisiana around 0800 UTC and lasted roughly 12 hours. Published studies based on geostationary data indicate that the actual cirrus coverage generated by persistent contrails might be as large as a factor of ten times

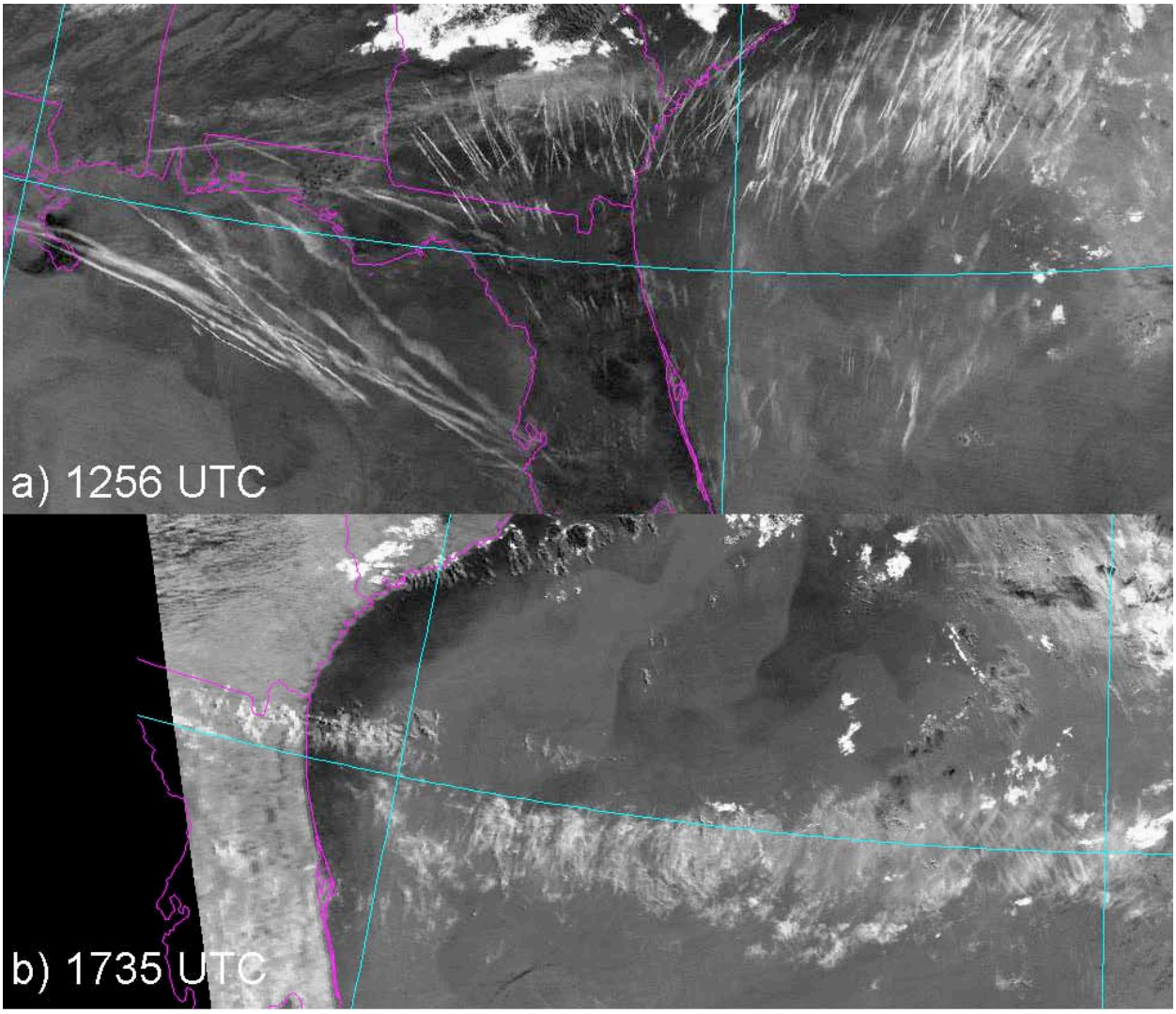

Figure 11 AVHRR T11 – T12 images from (a) NOAA-16 and (b) NOAA-19.

the coverage estimated for younger, linear contrails. Other studies based on trends in cirrus cloud cover suggest that the coverage including the linear contrails is most likely to be between 1 and 4. Determination of contrail coverage and evaluation of the resulting changes in cirrus cloud amounts are topics of ongoing research.

Another approach to estimating the total change in cloud cover due to contrails is through modeling, which has been undertaken at various levels of complexity and detail. Typically a model will use flight track distances within an atmospheric specified volume or other measures

of air traffic and simulate the production of contrails either by explicitly forming contrails and spreading them using a parameterization that differentiates them from natural cirrus or by adding cirrus to the atmosphere in proportion to the flight densities. Observations are often used to guide and/or validate these approaches.

Figure 12 shows an example of contrail and contrail-cirrus coverage estimated using a fairly sophisticated model. In this case, the coverage is broken down according to the derived contrail optical depth and age. Contrail-cirrus coverage is greatest over the northern hemisphere, especially over the North Atlantic, Europe, and the USA (**Fig. 12a**), regions with considerable air traffic. Europe is downwind of the Atlantic corridor and receives contrail-cirrus advected from that area. The heavier traffic over the USA and Europe lead to significant coverage by young contrails (< 5-h old), as seen in **Fig. 12b**. The model indicates that most of the contrail-cirrus coverage is due to very thin cirrus having optical depths < 0.02 (**Fig. 12c**). These very thin contrail cirrus clouds would be difficult to detect visually from the surface or with passive imagery. Younger contrails comprise a larger proportion of the contrail-cirrus coverage in the southern hemisphere than over the north where some areas (e.g., Russia, northern Canada) have negligible coverage due to young contrails (**Fig. 12d**). Not shown are the areas where significant decreases in natural cirrus occurred in the model as result of moisture being locked up in contrail cirrus. For example, the largest drops in natural cirrus coverage occurred over the eastern USA, Europe, and the northwest coast of Africa. Although the results discussed here have not been validated to date, they reveal the complexity of the problems faced in quantifying contrail impacts on cloudiness. Other models have produced different results and more research is needed to determine how accurately each model represents the actual atmospheric conditions.

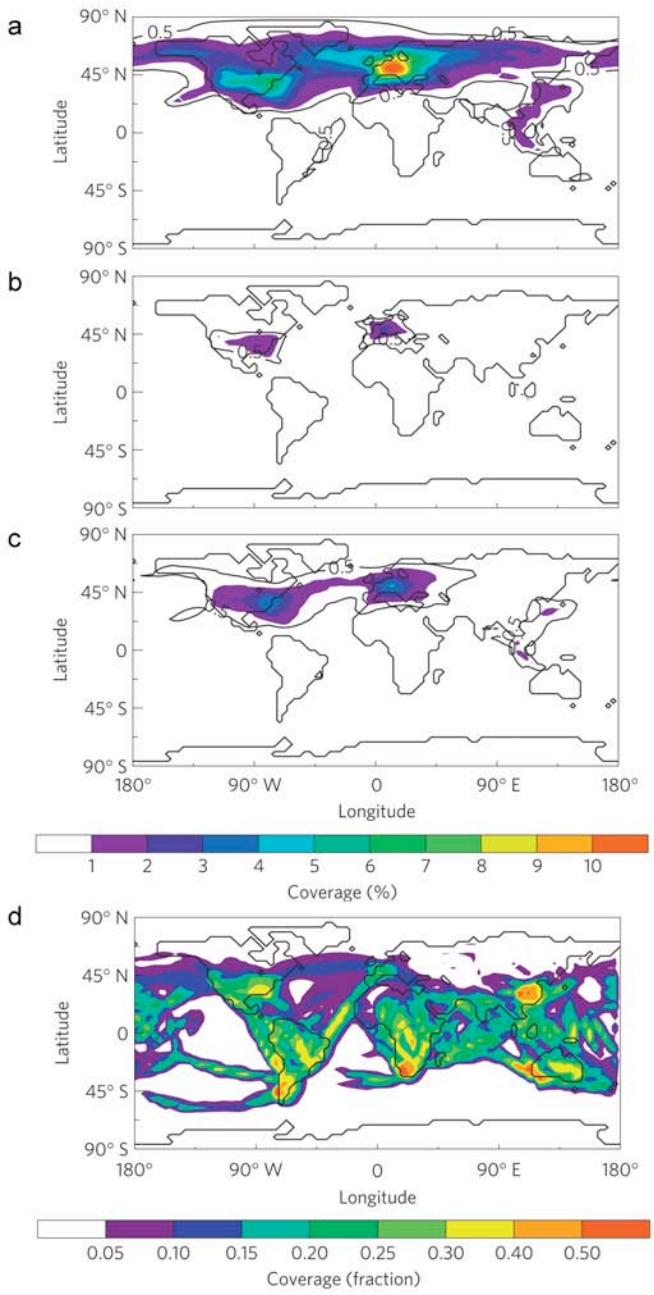

Figure 12 Average 2002 contrail cirrus and young-contrail coverage as simulated by ECHAM4-CCMod. Coverage due to (a) contrail cirrus, (b) persistent young contrails up to 5-h old and (c) visible contrail cirrus with optical depth > 0.02. (d) Fraction of contrail cirrus due to contrails up to 5-h old. Coverages computed assuming maximum overlap among contrails or contrail cirrus alone. Only part of the contrail/contrail cirrus coverage leads to increased overall cloud coverage. (Adapted from Figs. 1 and 2 of Burkhardt and Kärcher (2011) with permission.)

6.0 Contrail Climate Effects

Contrails, like other cirrus clouds, can affect both the hydrological and radiation budgets. Many of the possible contrail effects have only been the subjects of educated speculation, although some have been estimated to some degree. Some of these potential effects are mentioned here.

As noted earlier, by freezing out water vapor prior to the natural formation of cirrus clouds, contrails can alter the overall distribution of cirrus. Contrail formation may decrease precipitation in some clouds by reducing the average particle size in the affected clouds. Conversely, the precipitation induced by persistent contrails in otherwise clear air (e.g., **Fig. 3a**) may result in moistening of the middle layers of the troposphere and drying of the atmosphere at flight altitudes.

As a thin cirrus cloud, contrails reflect some solar or shortwave radiation that would otherwise warm the surface and absorb outgoing infrared radiation that cools the surface-atmosphere system. The overall radiative impact depends on the contrast between the contrail and its background, the lifetime of the contrail, and the solar zenith angle when it is present. Depending on the solar zenith angle and the thermal and albedo contrasts between the contrail and background, either surface or lower clouds, the net forcing can result in cooling or warming of the system. For instance, if the contrail forms over a dark background during midday, the amount of reflected sunlight may exceed the amount of infrared radiation blocked and reradiated by the cloud. Conversely, if it develops over a bright hot surface (i.e., desert) during the day, a contrail may reflect little additional solar radiation, but trap a significant amount of infrared because it is so much colder than the surface. Its overall impact would be substantially different than that over the dark surface. A similar effect would occur for a contrail over a warm low

cloud deck. At night, contrails warm the atmosphere. However, even during the day when solar and infrared forcing can almost cancel each other, the contrail will still impact the radiation field because most of the blocked sunlight results in cooling of the surface, while much of the infrared or longwave radiation "trapped" by the contrail warms the upper troposphere and has little immediate impact on the surface. Currently, 60% of air traffic is estimated to occur during the daytime.

These radiative forcing effects have been estimated with several different models and assumptions resulting in a minor amount of global warming when averaged over a long time period or some slight cooling on an instantaneous basis. **Figure 13**, which presents results from a general circulation model study, shows the distributions of linear contrail radiative forcings assuming random contrail cloud overlap, an average contrail particle effective diameter of 30 μm, and an optical depth of 0.2. This estimate is based on air traffic for 2002. The mean radiative forcings (RF) for contrails in otherwise clear skies are shown on the left half of the figure, while on the right are those for all skies, including both cloud-free backgrounds and clouds computed within the model. Positive RF indicates warming and conversely, negative forcing denotes a cooling effect. The greatest longwave (LW) RF for clear skies occurs over the eastern USA (**Fig. 13a**) where it exceeds 100 mWm^{-2}. **Figure 13b** shows that the LW RF is reduced by roughly a factor of two when clouds are included in the calculations. The shortwave (SW) RF is negative everywhere and strongest for cloud-free skies (**Fig. 13c**) over the eastern USA and Europe where it exceeds 500 mWm^{-2}. Inclusion of the clouds reduces the global SW RF by 60% to -3.8 mWm^{-2} (**Fig. 13d**). Combining the SW and LW forcings yields a net RF of 12.9 mWm^{-2} for clear skies (**Fig. 13e**) and 7.7 mWm^{-2} for the all sky case (**Fig. 13f**). While the

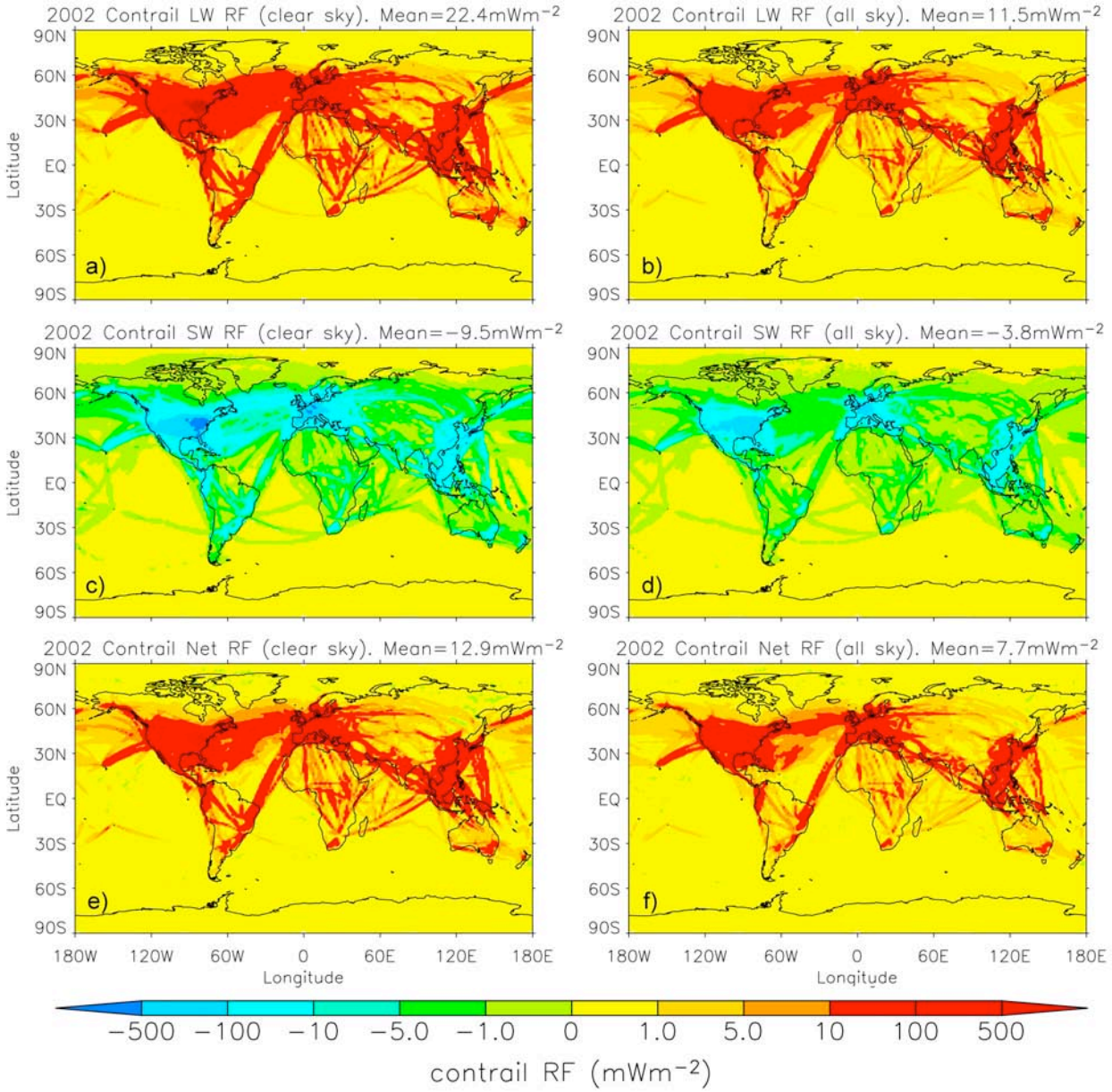

Figure 13 Radiative forcing (mWm^{-2}) at the top of the atmosphere for 2002 air traffic. (a, b) Longwave , (c,d) shortwave, and (e, f) net for (left) clear-sky forcings and (right) for all-sky forcings. Adapted from Rap et al. (2010) and reprinted with permission.

net RF is positive over most regions, negative net RF is seen over a few areas in the Arctic, central tropical Pacific, and over northeastern Asia.

This example is one of many computed in various ways during the last two decades. Various scenarios by other researchers have yielded net RF values between 0.0004 and 0.020 Wm^{-2} or more depending on many factors and the ways the model treats contrails and clouds. For

example, use of a different approach to account for clouds in the model calculations performed for **Figure 13** yields 12.0 mWm^{-2}. The best estimate of global net RF from linear contrails as of 2009 for the year 2005 is 11 mWm^{-2} with 90% confidence range from 5 to 25 mWm^{-2}. Yet, the scientists producing such estimates recognize that the level of scientific understanding remains low for such estimates. Even less understanding and confidence accompanies estimates of contrail cirrus RF, which ranges from 11 to 87 mWm^{-2}. To put these results in perspective, the linear contrail RF constitutes roughly 20% of all aviation RFs excluding that from contrail cirrus, including those from ozone carbon dioxide, water vapor, and nitrogen compounds. The 2005 best estimate of RF for all aviation, however, is only about 4% of all estimated anthropogenic radiative forcing if contrail cirrus is not included and could be 5% if it were included.

Since air traffic is expected to increase steadily in the coming decades, the same models used to estimate contrail RF for past or present air traffic have been employed to compute the contrail RF for the future. Based on several scenarios of technology and air traffic changes, climate models estimates of mean linear contrail net RF range from 37 to 55 mWm^{-2} for the year 2050. Inclusion of contrail cirrus boosts the contrail/contrail cirrus RF estimates up to as high as 315 mWm^{-2}. Current uncertainties in contrail coverage, optical depth, lifetimes, overlap with lower clouds, and other factors preclude a definitive assessment of the overall contrail impact. Despite these uncertainties, it is clear that, whatever effect they currently have on climate, it will increase in the future.

7.0 The Future

Contrails are difficult to study because of their high altitude, large advection rates, and frequent association with natural cirrus. Thus, current estimates of their impact are highly

uncertain. Nevertheless, their potential for affecting the global climate and providing military intelligence has spurred more interest and focused research into their formation, dissipation, microphysical and morphological characteristics, and methods for suppressing them. Removal of fuel sulfur or use of liquid hydrogen fuels have been suggested as means for diminishing the number of cloud nuclei and, hence, the number of contrails. Tests and theoretical studies have shown that such measures would probably not reduce the frequency of contrails. Hydrogen fuels would cause larger increases in local relative humidity in the exhaust plume causing higher supersaturations than would occur with hydrocarbon fuels. Thus, liquid hydrogen would probably cause more contrails to form, but possibly with greater particle sizes and fallout rates resulting shorter lifetimes and less radiative impacts. It is possible that a propulsion source that does not require exhaust of water vapor will be necessary to effectively eliminate the generation of contrails from high-flying aircraft.

Other methods to minimize contrail formation would involve changes in flight altitude or path. Contrail coverage could be reduced dramatically by flying in the stratosphere where contrail formation conditions are rare. However, other effects from the exhaust and increased fuel usage may limit the amount of stratospheric traffic. Flying at lower altitudes would diminish the number of contrails in tropical areas, but would cause additional coverage in the midlatitudes and polar regions. Conversely, higher mean flight altitudes would decrease contrails over the poles and temperate zones while causing more contrails in the equatorial areas. Ideally, numerical weather prediction models and contrail formation prognostication programs could be used together with flight planners to map out for each destination a sequence of flight altitudes that best avoids contrail formation conditions. Such planning could theoretically be used to neutralize the warming effect contrails or even induce a small cooling. Such sophisticated

planning would require more accurate temperature and humidity data and contrail prediction schemes than currently available as well as a more complex air traffic control network. Future research may provide the tools to minimize the climatic effects of contrails, but it is likely that these artificial clouds will be a common feature in the sky for many years to come.

See also: **Clouds, Cloud micro physics, Aerosols role in cloud physics, Aircraft emissions, Cirrus clouds, Climate radiative aspects, Cloud-radiative interactions, Human impact of climate change, Optical remote sensing, Rainbows, halos, and mirages, Satellite remote sensing of cloud properties, Thermodynamics of saturated air**

Further Reading

Brasseur G and M Gupta (2010) Impact of aviation on climate. *Bulletin of the American Meteorological Society*, 91, 461-463.

Burkhardt, U and B Kärcher (2011) Global radiative forcing from contrail cirrus. *Nature Climate Change*: 1, 54-58.

Duda, D P, P Minnis, L Nguyen, and R Palikonda (2004) A case study of contrail evolution over the Great Lakes. *Journal of the Atmospheric Sciences*: 61, 1132-1146.

Fahey, D W, U Schumann, S Ackerman, et al. (1999) Aviation-produced aerosols and cloudiness. Chapter 3 of IPCC Special Report: *Aviation and the Global Atmosphere*. Cambridge University Press, pp. 65-120.

Forster, P, V Ramaswamy, P Artaxo, et al. (2007). Changes in atmospheric constituents and in radiative forcing. Fourth Assessment Report of Working Group I of the Inter-governmental Panel on Climate Change. In: *Climate Change*. Cambridge University Press, UK.

Freudenthaler, V, F Homburg, and H Jäger (1995) Contrail observations by ground-based scanning lidar: cross-sectional growth. *Geophysical Research Letters*: 22, 3501-3504.

Heymsfield, A J, A Bansemer, G Thompson, et al. (2011) Formation and spread of aircraft-induced holes in clouds. *Science*: 333, 77-81.

Lee, D S, G Pitari, V Grewe, et al. (2010) Transport impacts on atmosphere and climate: Aviation. *Atmospheric Environment*: 44, 4,678-4,734.

Kärcher, B, B Mayer, K Gierens, et al. (2009) Aerodynamic contrails: Phenomenology and flow physics. *The Journal of Atmospheric Research*: 66, 217-226.

Mannstein, H, P Spichtinger, and K Gierens (2005) How to avoid contrail cirrus. *Transportation Research*: D10, 421–426.

Meyer, R, H Mannstein, R Meerkötter, U. Schumann, and P Wendling (2002) Regional radiative forcing by line-shaped contrails derived from satellite data. *Journal of Geophysical Research*: 107, 1-16.

Minnis, P, J K Ayers, R Palikonda, and D N Phan (2004) Contrails, cirrus trends, and climate. *Journal of Climate*: 17, 1671-1685.

Myhre, G, and F Stordal (2001) On the tradeoff of the solar and thermal infrared radiative impact of contrails. *Geophysical Research Letters*: 28, 3119–3122.

Rap, A, P M Forster, A Jones, et al. (2010) Parameterization of contrails in the UK Met Office Climate Model. *Journal of Geophysical Research*: 115, D10205, doi:10.1029/2009JD012443.

Ryan, A C, A R MacKenzie, S Watkins, and R Timmis (2011) World War II contrails: a case study of aviation-induced cloudiness. *International Journal of Climatology*: doi: 10.1002/joc.2392, 9 pp.

Sausen, R, I Isaksen, D Hauglustaine, et al. (2005) Aviation radiative forcing in 2000: An update on IPCC (1999), *Meteorologische Zeitschrift*: 14, 555 - 561, 10.1127/0941-2948/2005/0049.

Schumann U (1996) On conditions for contrail formation from aircraft exhausts. *Meteorologische Zeitschrift*: 5, 4-23.

Toon O B et al. (1996) Subsonic Aircraft: Contrail and Cloud Effects Special Study. *Geophysical Research Letters*: 25, 1109-1168.

Unterstrasser, S, and I Sölch (2010) Study of contrail microphysics in the vortex phase with a Lagrangian particle tracking model. *Atmospheric Chemistry and Physics*: 10, 10,003-10,015.

Voigt, C, U Schumann, T Jurkat, et al. (2010) In-situ observations of young contrails- overview and selected results from the CONCERT campaign. *Atmospheric Chemistry and Physics*: 10, 9,039-9,056.